Role of Sphingosine Kinase/S1P Axis in ECM Remodeling of Cardiac Cells Elicited by Relaxin

Alessia Frati,* Barbara Ricci,* Federica Pierucci, Silvia Nistri, Daniele Bani, and Elisabetta Meacci

Department of Biomedical, Experimental, and Clinical Sciences (A.F., B.R., F.P., E.M.), Research Unit of Biochemistry, and Department of Experimental and Clinical Medicine (S.N., D.B.), Research Unit of Histology and Embryology, University of Florence, 50134 Florence, Italy

The initiation and progression of heart failure is linked to adverse cardiac remodeling of the extracellular matrix (ECM) during disease mainly through the deregulation of myocardial metalloproteinases (MMPs). Relaxin (RLX), a peptide hormone acting as a physiological cardiac effector, is a key regulator of ECM remodeling in reproductive and nonreproductive tissues. Studying primary cultures of mouse cardiac muscle cells and rat H9c2 cardiomyoblasts, we have obtained evidence for a new signaling pathway activated by RLX to induce ECM remodeling that involves the bioactive sphingolipids sphingosine-1-phosphate (S1P) and ceramide. In both cell populations, recombinant human RLX increased sphingosine kinase activity and S1P formation, whereas sphingomyelin and ceramide content were decreased in [^{3}H]serine-labeled cells. According to the literature, RLX promoted MMP-2 and MMP-9 expression/release. Pharmacological inhibition of sphingolipid metabolism and silencing of sphingosine kinase 1, the enzyme responsible for S1P formation, were able to prevent MMP expression/release elicited by the hormone and induce the expression of tissue inhibitor of MMPs. In addition, we found that sphingolipid signaling is required for the regulation of connective tissue growth factor, a member of the CCN 1–3 family of genes that are involved in cell proliferation and differentiation. Finally, the induction of cardiomyoblast maturation induced by RLX was also found to be counteracted by inhibition of S1P formation. In conclusion, these findings provide a novel mechanism by which RLX acts on cardiac ECM remodeling and cardiac cell differentiation and offer interesting therapeutic options to prevent heart fibrosis and to favor myocardial regeneration. (*Molecular Endocrinology* 29: 53–67, 2015)

Bioactive sphingolipids (SLs), mainly ceramide and sphingosine-1-phosphate (S1P), are lipid mediators generated from the phospholipid precursor of cell membranes, sphingomyelin (SM) (1), by the action of several sphingomyelinases (SMases) (2). Ceramide can be also formed by de novo synthesis beginning with the condensation of L-serine and palmitoyl coenzyme A by serine palmitoyltransferase. The deacylation of ceramide leads to the formation of sphingosine (Sph), which can be phosphorylated by sphingosine kinase (SphK) activity to S1P (2, 3).

The bioactive lipid S1P has been suggested to mediate cell proliferation, differentiation and adaptation to adverse conditions, thus playing a central regulatory role in health and disease (1, 4, 5). In particular, evidence has been provided that S1P, by binding to multiple G protein-coupled receptors of the endothelial differentiation gene (*Edg*) family, currently named $S1P_{1-5}$ (1), regulates the migration, proliferation, and survival of endothelial cells. Moreover, S1P was reported to activate matrix metalloproteases (MMPs), particularly MMP-2, playing a key role in endothelial cell migration and angiogenesis (6).

S1P has also been shown to promote the relocalization of membrane-associated membrane type 1 (MT1)-MMP (MMP-14) to peripheral actin-rich membrane ruffles at the leading edge of bone marrow-derived stromal cells required for cell migration (7). Conversely, the other bioactive SL, ceramide, was reported to play opposite functions to S1P; for instance, in keratinocytes, ceramide induces a fibrogenic phenotype, because it stimulates the expression of TGF-β, elastin, MMP-1, and MMP-9, whereas MMP-2 was not affected (8).

MMPs are a family of more than 25 species of zinc-dependent proteases essential for the remodeling of extracellular matrix (ECM), a key event underlying a broad variety of physiological and pathological processes (9). MMPs are regulated at multiple levels including transcription, expression, secretion, and activation from inactive zymogens, and their activity is under the strict control of specific inhibitors, named tissue inhibitors of MMPs (TIMP). Aberrant expression of MMPs has been reported in several diseases, including cancer infiltration and metastasization, angiogenesis, inflammation, arthritis, pulmonary emphysema, multiple sclerosis, chronic wounds, and heart failure (6, 10). Among the MMPs expressed in the heart (reviewed in Ref. 11), MMP-2 and MMP-9, which are responsible for degradation of type IV collagen, the major component of basement membranes, appear to play an important role in adverse myocardial remodeling. In fact, increased gelatinases were found in both experimental and clinical heart failure (9, 12), whereas their deficiency in gelatinase-null mice was shown to prevent cardiac rupture and attenuate left ventricular enlargement and collagen accumulation after acute myocardial infarction (MI) (9, 13).

Notably, stimulation of ECM turnover and modulation of MMP expression and activity is a hallmark of the biological effects of the hormone relaxin (RLX) (14, 15). This is a member of the RLX peptide family which, in humans, encompasses 3 forms of RLX (H1, H2, and H3) and 4 insulin-like peptides (INSL-3 to -6) (16). Of these, H2 RLX, chiefly produced by the corpus luteum, is the main circulating hormone (16). The ECM-remodeling effects of RLX have been well documented in several organs and are mediated by its ability to inhibit profibrotic cytokine (primarily TGF-β1) signal transduction and hence the ability of these profibrotic factors to promote myofibroblast differentiation and subsequent myofibroblast-mediated ECM synthesis, deposition, and accumulation (17). Additionally, RLX stimulates a net increase in ECM degradation by promoting the actions of various MMPs, including MMP-1, MMP-2, and MMP-9 (17, 18), while inhibiting TIMPs. These combined actions of the hormone have collectively contributed to its development as a po-

tential antifibrotic agent. Recent in vitro studies using human (19) and rodent (20) fibroblasts have demonstrated that RLX disrupts TGF-β1 activity by interfering with its signal transduction at the level of Smad2 phosphorylation, as a means of inhibiting TGF-β1-induced myofibroblast differentiation, ECM production, and regulation of MMP activity.

The ability of RLX to increase ECM turnover by stimulating MMP expression/secretion is crucial to its physiological roles, especially in the cardiovascular system. In fact, it has been shown to be produced by the heart (21), to act on specific heart receptors (16), and to exert specific effects on the cardiovascular system, including coronary vasodilatation and neoangiogenesis (14, 22, 23).

A prominent role of RLX in cardiac diseases is also emerging. In fact, studies in RLX-null mice have demonstrated an age-related increase of fibrosis in the heart that can be reversed by H2 RLX administration (14, 24). In humans, myocardial upregulation of RLX expression has been reported in heart failure patients and interpreted as a compensative mechanism to sustain impaired cardiac function (21). In keeping with these findings, a recent phase III clinical trial on a cohort of patients with congestive heart failure has offered preliminary albeit convincing evidence that iv administration of recombinant H2 RLX can improve some key parameters of cardiac function and enhance the odds of survival (25, 26).

Although the ability of RLX to increase ECM turnover by stimulating MMPs expression/secretion is crucial to its physiological roles, the complex mechanisms whereby the hormone achieves these effects remain to be completely elucidated. Moreover, no data are yet available on the ability of RLX to regulate the expression of connective tissue growth factor (CTGF). This is a member of the cysteine-rich 61/CTGF/nephroblastoma overexpressed (CCN 1–3) family of genes (CCN family), which are operating in key biological processes such as cell proliferation, differentiation, adhesion, migration, and survival (27–29).

Based on the above reported similarities between the effects of S1P and RLX on MMP modulation, we hypothesized that bioactive SLs may be involved in the response of cardiac muscle cells to RLX.

In the present study, we provide the first evidence that RLX can activate SphK and upregulate S1P production in primary culture of mouse neonatal cardiac muscle cells and in rat H9c2 cardiomyoblasts. In addition, we show that the induction of SL metabolism and the decrease in S1P and ceramide synthesis triggered by RLX play a key role in the mechanisms presiding over MMPs and CTGF expression/release as well as cardiac muscle cell proliferation/differentiation.

Materials and Methods

Cell culture and treatment

Primary cultures of mouse ventricular cardiac muscle cells were prepared from hearts of 1- to 2-day-old newborn Swiss mice (Harlan) and cultured as previously described (30). Isolated primary cardiac muscle cells were used for the first 2 weeks (passages 0–1). Rat H9c2 cardiomyoblasts were from American Type Culture Collection. Both cell populations were incubated in serum-free essential medium overnight before treatment with the indicated concentrations of recombinant H2-RLX (Connetics Co) and/or inhibitors. PD98059, specific inhibitor of MAPK, SB202190, a highly selective, potent, and cell-permeable inhibitor of p38 MAPK (Tocris Bioscience). SL metabolism enzyme inhibitors used in the study were GW4869, a cell-permeable, noncompetitive inhibitor of neutral SMases (31, 32) and SKI-II, selective nonlipid inhibitor of SphK (33), were from Tocris Bioscience. THI, inhibitor of S1P lyase (34) was obtained from Sigma-Aldrich s.r.l.

SphK activity measurement

SphK activity was determined essentially as described previously (35, 36). Briefly, equal amounts of protein (60 μg) from primary cardiac muscle cells and H9c2 cells were incubated in assay buffer in the presence of 20 μmol/L Sph and 200 mmol/L [^{32}P]ATP (3 μCi/assay). SphK activity was measured in a typical buffer solution for detecting mainly SphK1 isoform activity. Reactions were started with the addition of lysate proteins and incubated for 30 minutes at 37°C. The formed [^{32}P]S1P in the organic phase was separated by TLC on Silica Gel 60 using $CH_3(CH_2)_3OH/ CH_3COOH/H_2O$ (3:1:1, vol:vol) (37). The radioactive spots corresponding to authentic S1P were identified and quantified by scraping from the plates and counting the radioactivity in a Beckman LS1000 counter.

Quantification of cellular SLs in primary cardiac muscle cells

SLs were quantified essentially as previously described in De Palma et al (38). Cardiac muscle cells were incubated with serum-free medium and 2 μCi of [^{3}H]serine for 24 hours. Total lipids were extracted by the addition to cells of $CHCl_3$: CH_3OH: HCl (100:200:1, vol:vol). The lower phase was evaporated and lipids separated by TLC on Silica Gel 60 with $CH_3(CH_2)_3OH/ CH_3COOH/H_2O$ (3:1:1, vol:vol). The radioactive spots corresponding to S1P were identified and quantified as described above.

RT-PCR analysis

To evaluate the expression levels of mRNA for Relaxin/insulin-like family peptide receptor 1 (RXFP1), RT-PCR was performed using mouse cardiomyocytes and rat H9c2 cells. Mouse and rat atria, which constitutively express *RXFP1*, were used as positive controls. Total RNA was isolated by extraction with TRIzol reagent (Invitrogen) according to the manufacturer's instructions. To avoid genomic DNA contamination, the samples were treated with 2 to 10 U deoxyribonuclease (DNase) I (Roche Diagnostics or Invitrogen). TIMP-1 amplification using untreated RNA and DNase-treated RNA is reported (note the presence of a higher band corresponding to an amplified intron region indicating the contamination by genomic DNA). One

microgram of total RNA was reverse transcribed and amplified with the SuperScript One-Step RT-PCR System (Invitrogen). After cDNA synthesis for 30 minutes at 55°C, the samples were predenatured for 2 minutes at 94°C and then subjected to 38 cycles of PCR performed at 94°C for 15 seconds, alternating with 55°C for mouse *RXFP1* and 57°C for rat *RXFP1* for 30 seconds and 72°C for 1 minute; the final extension step was performed at 72°C for 5 minutes. The following specific primers were used: mouse *RXFP1* (NM_212452.1) forward 5′-ACG AGC TGT CCC ATC AGT TT-3′ (354–372 bp) and reverse 5′-ATG TGC TGA CAG AGG GGT TT-3′ (718–737 bp) (transcript length 383 bp); rat *RXFP1* (NM_ 201 417.1), forward 5′-CGG ATG GGA TCT CCT CTC TT-3′ (1178–1197 bp) and reverse 5′-GCG TGC TTC CTG TAC TCT CC-3′ (1408–1427 bp) (transcript length 249 bp). Both primers were designed to span an intron. Negative controls, consisting of no template (water), were performed in each run. PCR products were electrophoresed on a 2% agarose gel.

To evaluate the expression of S1P receptor subtypes, total RNA from cardiomyocytes and H9c2Cells were isolated by extraction with TRI Reagent (Sigma-Aldrich, s.r.l.), according to the manufacturer's instructions. Concentration and purity of extracted total RNA were evaluated by measuring the absorbance at 260 and 280 nm wavelength and the absence of degradation confirmed by agarose gel electrophoresis with ethidium bromide staining.

One microgram of total RNA from H9c2 and primary cardiac muscle cells were reverse-transcribed to single-stranded cDNA using the commercially available cDNA Synthesis Kit (SuperScript III cells Direct cDNA Synthesis Kits; Life Technologies) or SuperScript One-Step RT-PCR System (Invitrogen) according to the manufacturer's instructions. Mouse C2C12 cells, which constitutively express S1P1, S1P2, and S1P3 were used as positive controls. Samples were incubated at 70°C for 10 minutes, 25°C for 15 minutes, 42°C for 60 minutes, and then 70°C for 5 minutes in a thermal cycler (PerkinElmer). To amplify S1P receptor subtypes, we chose forward and reverse primers in a region of nucleotide sequences identical in rat and mouse genes: *S1P1* (NM_007901), *S1P2* (NM_010333), and *S1P3* (NM_007901). Because the coding region covers a single exon, to avoid genomic DNA contamination, the samples were treated with 10 U DNase I (Roche Diagnostics). The primers were designed as follows: *S1P1* forward 5′-CCG CAA GAA CAT CTC CAA GG-3′ (711–730 bp) and reverse 5′-GGC AAT GAA GAC ACT CAG GA-3′ (782–801 bp) (transcript length 91 bp); *S1P2* forward 5′-CAT CGT GGT GGA GAA TCT TCT G-3′ (138–159 bp), and reverse 5′-CAG GTT GCC AAG GAA CAG GTA-3′ (203–225 bp) (transcript length 88 bp); and *S1P3* forward 5′-CCA CCT GCA GCT TAC TGG CC-3′ (377–396 bp) and reverse 5′-GGC AAT TAG CCA GCA CAT CCC-3′ (478–498) (transcript length 122 bp). For amplification of TIMP-1, MMP-2, and MMP-9, the primers were designed as following: rat *TIMP-1* (NM_053819.1) forward 5′-GAC CAC CTT ATA CCA GCG-3′ (162–179 bp) and reverse 5′-ACA CCC CAC AGC CAG CAC TA-3′ (429–448 bp) (transcript length 287 bp, with 2 introns 674 bp); rat *MMP-9* (NM_031055.1) forward 5′-TCG AAG CAG ACA TTG TCA-3′ (488–505 bp) and reverse 5′-TCG TCG TCG TCG AAG TGG GC (607–626 bp) (transcript length 139 bp); and rat *MMP-2* (NM_031054.2) 5′-TGA CGG CAA GGA CGG ACT C-3′ (552–570 bp) and reverse 5′-CTT GCA GTA CTC GCC

ATC-3′ (684–701bp) (transcript length 150bp). Negative controls for reverse transcription were performed using DNase-treated RNA and for PCR consisted of no template (water).
Real-time PCR.

Quantitative real-time PCR was carried out using the Rotor.Gene 6000 (Corbett Research, Corbett Life Science) and Sybr Green reagents (Life Technologies) consisting of a specific set of primers (200nM) and a fluorogenic internal probe. The expression of *S1PR* genes were quantitated in comparison with the housekeeping gene *GAPDH*. PCR amplifications were performed on cDNA samples corresponding to a final RNA concentration of 50 ng. PCR was performed in a total volume of 25 μL containing 2× PCR Master Mix (Life Technologies). Reaction conditions were as follows: 95°C for 10 minutes, followed by 35 to 40 cycles at 95°C for 30 seconds alternating with 52°C, 55°C. or 60°C for 30 seconds and 72°C for 45 seconds. PCR amplifications were run in duplicates.

Blank controls were performed in each run. The results of the real-time PCR were presented as cycle threshold (Ct) values, where Ct was defined as the PCR threshold cycle at which amplified product was first detected. All values were normalized to the *GAPDH* housekeeping gene expression and ΔCt calculated.

Cell silencing by short interfering RNA

To inhibit the expression of SphK1, a mix of short interfering RNA (siRNA) duplexes corresponding to 2 distinct regions of the DNA sequence of *SphK1* gene (SphK1-siRNA) was used as previously reported (35): *SphK1* siRNA1 (5′-GGG CAA GGC UCU GCA GCU CdTdT-3′) and SphK1-siRNA2, (5′-AAG GGC AAG CAU AUG GAA CdT dT-3′). H9c2 cells (200 000 cells per well) were transfected with a mix of both SphK1-siRNAs (100nM) using Lipofectamine 2000 reagent according to manufacturer's instructions. After 36 hours from the beginning of transfection, conditioned medium and cells were collected and used for the reported experiments. Nonspecific scrambled (SCR) siRNA was used as control. The specific knockdown of SphK1 was evaluated by Western blotting, and the efficiency of transfection was estimated as approximately 65% ± 8% (n = 3).

Gelatin zymography

MMP/collagenase activity was assessed by gelatin zymography from conditioned medium (30). Cells were analyzed after 24 to 48 hours in culture as indicated. In some experiments, primary cardiac muscle cells and H9c2 cardiomyoblasts were incubated for 30 minutes in the presence or absence of the specific compounds or inhibitors. After 24 hours, the conditioned medium was collected and centrifuged at 10 000*g* for 15 minutes and stored at −20°C. Samples, 10 to 20 μL each, were mixed with sample buffer and separated on 10% SDS-polyacrylamide gels containing gelatin (1 mg/mL), and gel was developed as reported previously (30). The MMPs appear as bright bands within the stained gel, and the clear bands indicate proteolytic activity. MMPs were identified by comparison with molecular weight standards.

MMP measurement by ELISA

Culture media obtained from the 24 hours of incubation of cardiac cells were thawed and used in the MMP-2/-9 ELISA (Boster Biological Technology Co Ltd), according to the manufacturer's protocols with minor modifications. The resultant reactions were read at a wavelength of 450 nm in a microplate Bio-Rad reader. Three independent experiments were carried out and duplicates of each sample were measured with the ELISA kit. Data (means ± SEM), reported as nanograms per milliliter, were calculated by interpolating the absorbance in a standard curve.

Western blotting analysis

To prepare total extracts, native and transfected cells were processed as previously described (39–41) Proteins (30 μg) from lysates or cellular fractions were subjected to electrophoresis (SDS-PAGE) and Western analysis as previously described (42). To immunodetect endogenous RXFP1, rabbit polyclonal antirelaxin receptor (RXFP; 1:3000; Immunodiagnostik) was used. Specific polyclonal anti-SphK1 antibodies from ECM Bioscience were used to evaluate the expression of SphK1, whereas rabbit polyclonal antibodies against amino acids 363 to 382 of human/rat connexin-43 (Cx43) (Sigma) were used for detecting the state of cardiac muscle cell differentiation. Anti-CTGF antibodies (PA5–32193 against amino acids115- 315 of human CTGF) to detect CTGF/CNN2 and TIMP-1 (mouse IgG1, clone 102D1) were from Merck Millipore. Bound antibodies were revealed by antirabbit, antimouse or antigoat IgG1 conjugated to horseradish peroxidase (Santa Cruz Biotechnology, Inc) and Enhanced chemiluminescence (ECL) reagents (Amersham Pharmacia Biotech). Rabbit polyclonal anti-SphK1 antibodies were from ECM Biosciences LLC. Anti–β-actin or anti–β-tubulin (Santa Cruz) was used to demonstrate the quality and equivalent loading of protein.

Cell proliferation analysis

Primary cardiac muscle cells were incubated for 24 hours in DMEM in the absence of the indicated compounds, and [³H]thymidine (2 μCi/mL) (PerkinElmer) was added to the medium for the last hour of incubation. Cells were processed as reported (36, 42), and the recovered radioactivity was measured in a β-counter (Beckman).

Statistical analysis

Representative zymographs or blots are reported. Densitometric analysis of the bands was performed using Imaging and Analysis Software by Bio-Rad (Quantity-One) or ImageJ (National Institutes of Health) software and reported as relative percentage (means ± SEM) obtained by calculating the ratio of the band intensity of the specific protein to β-actin or β-tubulin intensity and normalizing to control, set as 100. In zymographs, the amount of gelatinolytic activity of the control sample was arbitrarily set to 100% in each gel. The MMP activity of the samples was interpolated from the standards curve, and data from independent experiments performed in duplicates are reported as relative percentage above control (means ± SEM). In ELISA tests, MMP concentration is reported as nanograms per milliliter (means ± SEM). Statistical significance for all methodological approaches was determined by Student's *t* test or one-way ANOVA, with a value of $P < .05$ considered significant. At least 3 independent experiments were performed for the studies (zymographs and blots) involving primary cardiac muscle cells, whereas 4 to 6 independent experiments were carried out for the studies involving the H9c2 cells.

Results

RLX triggered SL metabolism

SL metabolism is involved in the signaling pathways of several hormones in many cell types (43). As in our previous studies (30, 44), we used primary cultures of mouse neonatal cardiac muscle cells to investigate the potential role of bioactive SLs in the typical cell responses to RLX. Upon isolation, they appear as scattered round or polyhedral cells. After 24 hours incubation, the cells formed rhythmically beating clusters (Supplemental Figure 1). The reported analyses were performed at this stage.

We first investigated whether RLX was able to modulate the activity of SphK, the enzyme responsible for S1P synthesis. Enzyme activity was measured on cell lysates obtained from both primary murine cardiac muscle cells and H9c2 cardiomyoblasts. As shown in Figure 1, RLX (50 ng/mL) induced a significant increase in SphK activity in both cell types, reaching a maximal stimulation at 15 minutes. At this time point, lower RLX doses (down to 10 ng/mL) were also efficient (data not shown). Because the enzyme activity assay was performed in a buffer without KCl, the $[^{32}P]$S1P formed during the assay can be chiefly attributed to the activation of SphK1 isoform (33). Notably, after long-term exposure (24 hours), RLX did not substantially increase the expression of SphK1 (Figure 1, inset), supporting the involvement of a posttranslation modification in enzyme activation.

Because it has been reported that the content of bioactive SLs is crucial for cell fate (1, 3, 35, 36, 38, 41), we then explored whether RLX changed the levels of SM and its distal metabolites, ceramide, Sph, and S1P, in primary cardiac muscle cells labeled with $[^3H]$serine. As shown in Figure 2, a significant increase in $[^3H]$Sph and $[^3H]$S1P formation was detected 15 and 30 minutes after RLX treatment, whereas $[^3H]$SM and $[^3H]$ceramide content were significantly reduced at these time points. Notably, S1P levels increased earlier than the levels of Sph, suggesting that as soon as $[^3H]$Sph is formed by $[^3H]$SM degradation, the lipid is rapidly phosphorylated to $[^3H]$S1P by activated SphK.
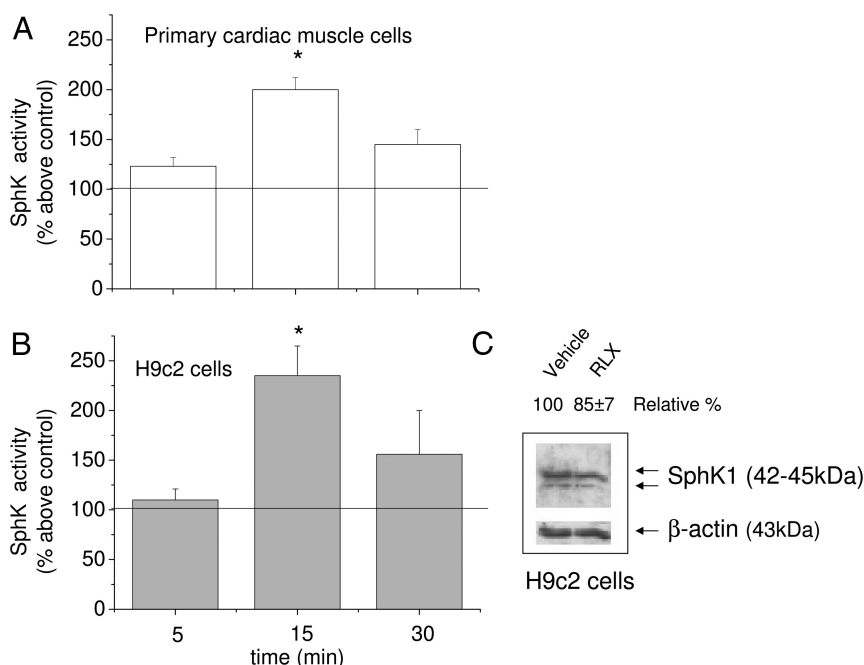
The classical signaling pathways activated by RLX in target cells, such as fibroblasts (45, 46), involve the activation of RXFP1/ERK1/2 signaling. Thus, because ERK1/2 has been reported to be crucial for SphK activation (2, 3), first we determined the expression of RXFP1 in H9c2 and primary cardiac muscle cells. Both cell populations express RXFP1 at the mRNA and protein level as demonstrated by RT-PCR analysis and Western blotting shown in Figure 3, A and B, respectively. Positive controls corresponding to murine heart tissue (atria) are also reported in the same figure.

Successively, we established the potential role of ERK1/2 and p38 MAPK and ERK in RLX-induced enzyme activation performing pharmacological inhibition of ERK1/2 by PD098059 and of p38 MAPK by SB202190 (Figure 3C). Of note, the RLX-induced activation of SphK was prevented by PD098059 as well as by U0126 (5μM), another recently identified MAP kinase kinase kinase (MEKK) inhibitor (Figure 3D), whereas SB202190 did not affect enzyme activity. Neither PD098059 nor SB202190 treatment significantly affected basal SphK activity.
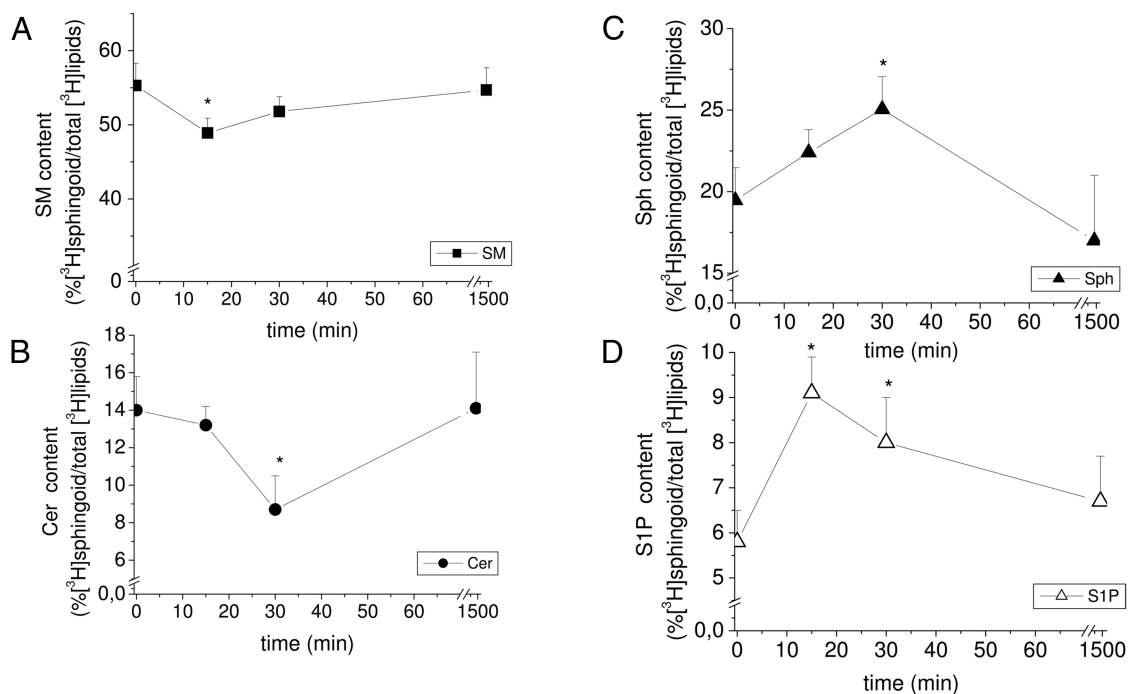
Altogether, these findings suggest that SM-derived bioactive SLs are novel effectors in the signaling pathways promoted by the RLX/ERK1/2 axis in cardiac cells.

Figure 1. RLX induces SphK activity in primary cardiac muscle and H9c2 cells. A and B, SphK activity was determined in cell lysates (30–50 μg) obtained from untreated primary cardiac muscle cells (A) and H9c2 cells (B) and cardiac cells treated with RLX (50 ng/mL) over the indicated time. Results are expressed as mean ± SEM of at least 3 independent experiments with analogous results performed in duplicate (Student's *t* test; *, *P* < .05). C, Representative Western blot of SphK1 isoform expression in H9c2 cells. Cell lysates (25 μg) were subjected to SDS-PAGE and SphK1 isoform immunodetected by specific rabbit polyclonal antibodies. Band intensity, reported as relative percentage of control, was arbitrarily normalized to 100 (mean of 3 experiments, SEM <15%).

S1P formation and de novo synthesis of ceramide are required for RLX-induced MMPs

Because RLX is known for its ECM-remodeling properties (14, 30),

Figure 2. RLX treatment promotes SL metabolism. Primary cultures of cardiac muscle cells were incubated for 24 hours with [³H]serine and then treated with or without RLX (50 ng/mL) for the indicated times. SLs were extracted as reported in Materials and Methods and ³H-radiolabeled SM (A), ceramide (B), sphingosine (C), and S1P (D) quantified as in *Materials and Methods*. SL content on total radiolabeled lipids is reported as mean ± SEM of at least 3 independent experiments (Student's *t* test; *, *P* < .05).

we then studied whether the bioactive SLs could be a part of the RLX-induced signaling leading to the induction of latent and active MMP expression/release. The conditioned medium obtained from both cell cultures treated or not with

RLX was used for gelatin zymography and ELISA to identify and quantify the gelatinases released by the cells. As shown in Figure 4, A–C, latent and active MMP-9 of 92 and 85 kDa, respectively, and active MMP-2 (72 kDa)
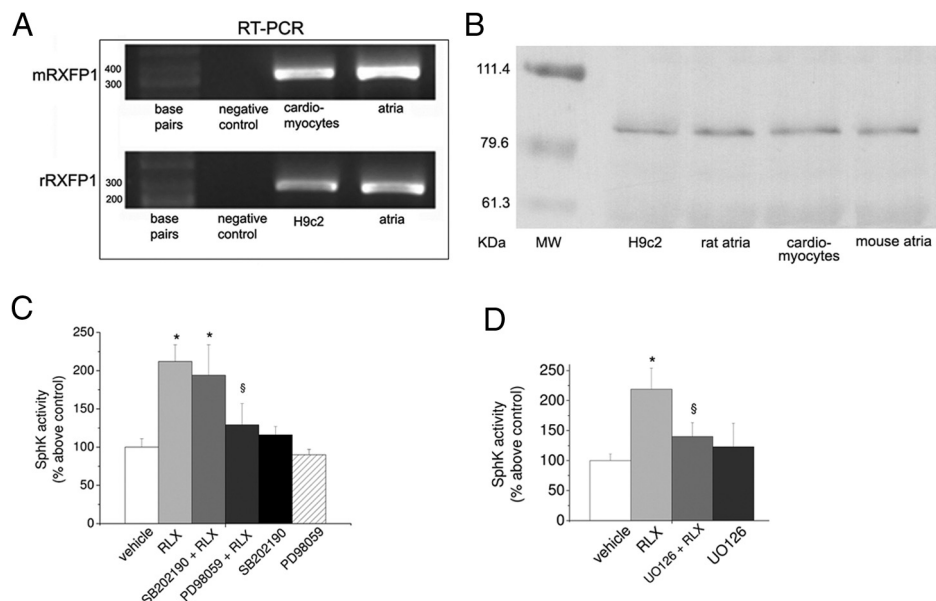
Figure 3. RLX receptor subtype expression and effect of ERK1/2 and p38 MAPK inhibitors on RLX-induced SphK activity. A, Representative agarose gel. Expression of RLX receptor subtype (RXFP1) mRNA in H9c2, cardiac muscle cells, and atria. RT-PCR was performed as in Materials and Methods from H9c2, cardiac muscle cells, and atria mRNA (2 μg). B, Representative Western blotting. RXFP1 was immunodetected by specific polyclonal antibodies in cell lysates (20 μg) of H9c2 and primary cardiac muscle cells and murine tissue (atria). C and D, ERK1/2 or p38 MAPK specific inhibitors PD98059 (15μM), UO126 (5μM), and SB202190 (10μM) were added to the cell medium alone or 30 minutes before RLX treatment. SphK activity was determined as described in Figure 1 and in Materials and Methods. Data are mean ± SEM of at least 3 independent experiments (Student's *t* test; *, *P* < .05 vs vehicle; §, *P* < .05 vs RLX).
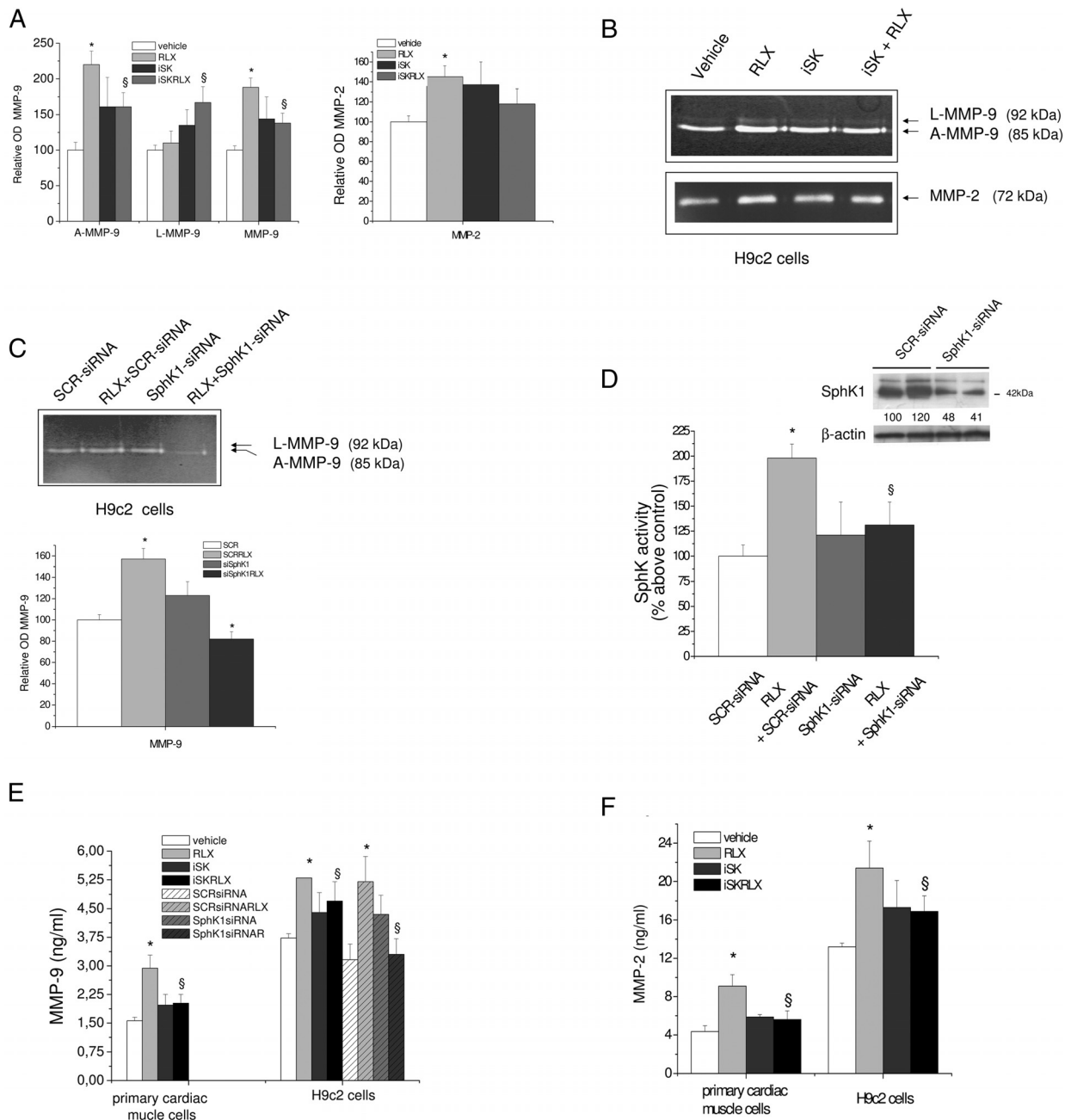
Figure 4. Inhibition of S1P synthesis on RLX-induced MMP-9 and MMP-2 release in primary cardiac muscle cells and H9c2 cells. A and B, A representative gelatin zymograph of latent (L) and active (A) MMP-9 and MMP-2 from conditioned media obtained from primary cardiac muscle cells (A) and H9c2 cardiomyoblasts (B) treated for 30 minutes with compound II (iSK, 5μM) before the addition of RLX (50 ng/mL) for another 24 hours. Densitometry scanning from at least 3 separate experiments for each cell type studied was performed, and data expressed as relative OD values (L-MMP-9, A-MMP-9, and overall MMP-9) to those of the untreated group (vehicle) set to 100, are reported in the graphics. Data are mean $\pm$ SEM (ANOVA test; *, $P < .05$ vs untreated cells (vehicle); §, $P < .05$ vs RLX). C, A representative gelatin zymograph of MMP-9 from conditioned media obtained from H9c2 cells transfected with 50nM scrambled (SCR-siRNA) or SphK1-specific siRNA (SphK1-siRNA) for 24 hours and then treated or not with RLX (50 ng/mL) for another 24 hours. Samples were analyzed as reported in Materials and Methods and statistical significance calculated as above. D, SphK activity. H9c2 cells transfected with scrambled (SCR-siRNA) or SphK1-specific siRNA (SphK1-siRNA) as in C were used for SphK activity assay and SphK1 protein expression analysis. Inset, Proteins from H9c2 cell lysate (30 μg) were separated by SDS-PAGE and blotted, and SphK1 was immunodetected using specific polyclonal antibodies as described in Materials and Methods. Data are mean $\pm$ SEM of 3 independent experiments performed in duplicate (Student's t test; *, $P < .05$). Relative percentage of SphK1 expression is indicated in the inset (SEM <15%). E and F, Conditioned cell media from primary cardiac muscle and H9c2 cells, incubated and treated as reported above, were analyzed by ELISA. Relative OD_{450nm} was measured by microplate reader and sample concentration interpolated using a standard curve. Two independent experiments in duplicate were carried out, and data are reported as percentage above control (vehicle). Data (nanograms per milliliter) are mean $\pm$ SEM (ANOVA test; *, $P < .05$ vs untreated cells (vehicle); §, $P < .05$ vs RLX).

were detected in the supernatants from both primary cardiac muscle cells and H9c2 cardiomyoblasts upon 24 hours of incubation. An RLX dose of 50 ng/mL was found effective in enhancing the release of either MMP-9 or MMP-2, and in both cell populations, the effect of RLX was prevented by incubating the cells in the presence of SphK inhibitor (compound II, iSK) (Figure 4, A and B). The involvement of the isoform SphK1 in RLX-induced MMP-9 release was demonstrated by SphK1 gene silencing in H9c2 cells. As reported in Figure 4, the transfection of H9c2 cells with SCR-siRNA or SphK1-siRNA for 24 hours strongly inhibited the release of MMP-9 promoted by RLX (Figure 4C) and significantly reduced SphK activity and enzyme expression of approximately 85% and 55%, respectively (Figure 4D and inset). The enhanced release of MMPs elicited by the cardiotropic hormone and the role of SphK inhibition in counteracting hormone action in cardiac cells was further confirmed by ELISA (Figure 4, E and F).

Altogether, these data demonstrate for the first time a correlation between the ability of RLX to promote ECM remodeling and the activation of the SphK/S1P axis.

To further investigate the involvement of SM-derived metabolites in the RLX-induced release of MMPs, we evaluated by zymography and ELISA the effects of other inhibitors of SL metabolism, namely GW4869, a noncompetitive inhibitor of neutral SMases (32), and THI, a rather specific inhibitor of S1P lyase (34). Before performing the zymography and ELISA, we tested the dose of S1P lyase, SMase, and SphK inhibitors. As reported in Table 1, quantification of mRNA encoding MMP-9, MMP-2, and TIMP-1 in untreated H9c2 cells or cells treated with the indicated concentrations of inhibitors (THI, GW, or iSK) and S1P. ΔCt revealed no significant effects of the treatment on RNA expression, indicating that the dose used to specifically inhibit S1P lyse, SMase, and SphK activity was not cytotoxic. The exogenous addition to the cell medium of the bioactive lipid, S1P, was also evaluated. As shown in Figure 5, A–C, zymography analysis indicated that, similarly to iSK, GW4869 treatment and exogenous addition of S1P led to a significant reduction of RLX-promoted release of MMP-9 (approximately 30% and 90%) in cardiac muscle cells as well as in H9c2 cells (Figure 6B). On the contrary, THI treatment was ineffective on either MMP-9 or MMP-2.

The correlation between SL mediators and MMP-9 release was further proven by a sensitive ELISA (Figure 5, C and D). Of note, the addition of exogenous S1P to cell medium strongly reduced the effect of RLX on MMP-9 release at similar extent than iSK alone, suggesting a role for the signaling downstream of the specific S1P receptors (3).

In keeping with these findings, we found that the expression of TIMP-1, the endogenous inhibitor of MMPs, was reduced approximately 45% by RLX (Figure 6A), and the treatment with SphK inhibitor, GW4869, or exogenous S1P, before hormone addition, significantly prevented its effect. On the contrary, no change was observed when the cells were treated with THI (Figure 6B).

RLX reduced CTFG expression through SL metabolism

CTGF (CCN2) is thought to play an important role in cardiac remodeling (28, 29). As shown in Figure 7A, RLX and the inhibitor of SphK significantly reduced the basal level of CTGF in primary cardiac muscle cells. Of note, the downregulation of CTGF elicited by RLX was further enhanced by SphK inhibition, whereas GW4869 and S1P treatment had no effect. On the contrary, in H9c2 cells, the addition of iSK to the culture medium significantly prevented hormone action, whereas the treatment with GW4869 and the exogenous addition of S1P further potentiated RLX-induced decrease of CTGF expression (Figure 7B).

Table 1. Effect of SphK, SMase, and S1P Lyase Inhibition and S1P Addition on MMP-9, MMP-2, and TIMP-1 Expression in H9c2 Cells[a]

	Control	**iSK**	**GW4869**	**THI**	**S1P**
MMP-9					
Ct	29.66	24.1	24.6	24.47	25.02
ΔCt	7.64 ± 0.8	6.76 ± 0.6	6.72 ± 0.7	5.57 ± 0.7	7.25 ± 0.7
MMP-2					
Ct	33.09	27.7	28.47	28.05	28.09
ΔCt	11.07 ± 1.0	10.38 ± 1.2	10.59 ± 1.0	9.15 ± 1.2	10.32 ± 1.1
TIMP-1					
Ct	31.75	25.74	26.61	26.4	25.87
ΔCt	10.5 ± 1.1	9.35 ± 1.0	9.18 ± 1.1	9.33 ± 1.1	9.21 ± 1.0

[a] MMP-9, MMP-2, and TIMP-1 expression was evaluated from RNA extracted from untreated H9c2 (control) cells and cells treated for 30 minutes with compound II (iSK, 5μM), GW9846 (10μM), THI (6.5μM), or S1P (1μM). Total RNA was reverse transcribed and real-time PCR amplification performed as described in Materials and Methods. ΔCt values are reported as mean ± SEM for independent experiments performed in duplicate. Significance of differences was tested by one-way ANOVA, and no significant change was observed in the presence of inhibitors vs control.
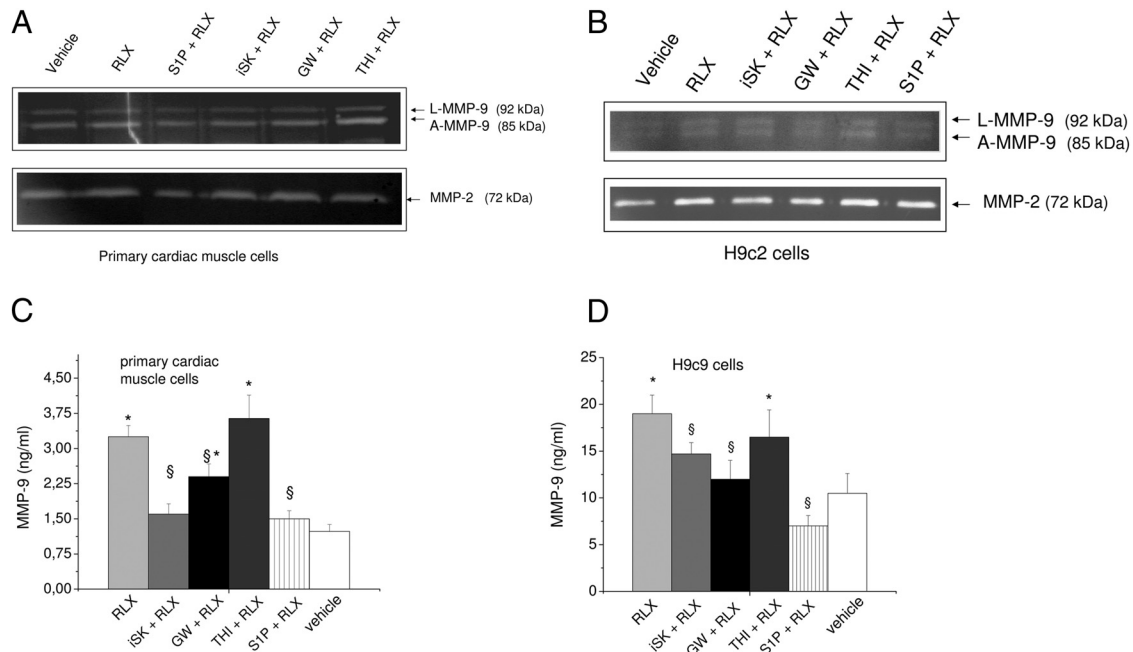
Figure 5. Effect of SphK, SMase, and S1P lyase inhibition and extracellular S1P addition on RLX-induced MMP-9 and MMP-2 activity in primary cardiac muscle cells and H9c2 cells. A and B, Representative zymographs of latent (L)-MMP-9, active (A)-MMP-9, and MMP-2 activity from conditioned media obtained from primary cardiac muscle cells (A) and H9c2 cardiomyoblasts (B) treated for 30 minutes with S1P (1μM), compound II (iSK, 5μM), GW9846 (10μM), or THI (6.5μM) and then incubated in the absence or presence of RLX (50 ng/mL) over 24 hours. Relative OD was determined by densitometry scanning and data as relative percentage to control (vehicle) arbitrarily normalized to 100 are reported in the graphics. Data are mean ± SEM of at least 3 independent experiments (Student's t test; *, $P < .05$ vs untreated cells (vehicle); §, $P < .05$ vs RLX). C and D, MMP-9 ELISA. Conditioned cell media obtained from primary cardiac muscle cells (C) and H9c2 cells (D) treated for 30 minutes with S1P (1μM), compound II (iSK, 5μM), GW9846 (10μM), or THI (6.5μM) and then incubated in absence or presence of RLX (50 ng/mL) over 24 hours. Samples were analyzed and data reported as nanograms per milliliter as described in Materials and Methods. Data are mean ± SEM of at least 3 independent experiments (Student's t test; *, $P < .05$ vs untreated cells (vehicle); §, $P < .05$ vs RLX).
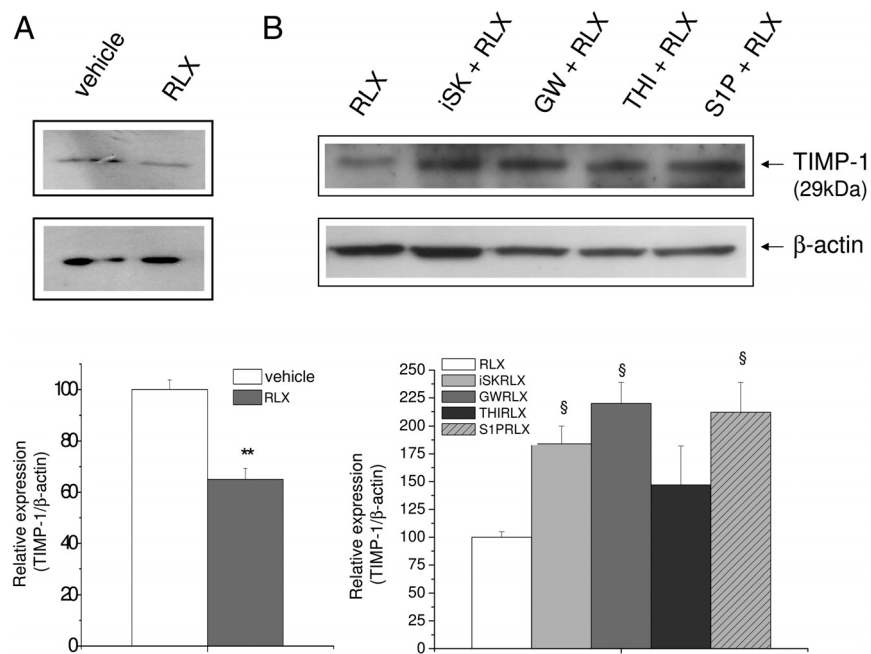
Therefore, by comparing the effects of iSK and S1P in primary cardiac muscle cells and H9c2 cells, we can hypothesize a different role for the intracellularly formed S1P and the signaling pathways induced by exogenous S1P at different stages of cell maturation. Notably, as reported in Figure 8, we found by RT-PCR analysis that the mRNA encoding $S1P_1$, $S1P_2$, and $S1P_3$ are specifically expressed in primary cardiac muscle cells (Figure 8D), whereas only $S1P_1$ and $S1P_2$ mRNA was detected in H9c2 cells (Figure 8E). Positive control corresponding to RT-PCR performed using RNA obtained from C2C12 myotubes that express all 3 S1P receptor subtypes is also reported (Figure 8C). Due to the low level of expression in primary cardiac muscle cells, the difference in S1P receptor subtype expression between the 2 populations were confirmed by real-time PCR. In Table 2, the Ct and ΔCt for $S1P_1$, $S1P_2$, and $S1P_3$ expression in primary cardiac cells and H9c2 cells is reported. Temperature of melting was equal to 79.91°C, 79.99°C, and 91.14°C for $S1P_1$, $S1P_2$, and $S1P_3$, respectively. Notably, real-time PCR analysis indicated a similar expression level of all 3 receptor subtypes in primary cardiac muscle cells and confirmed the lack of $S1P_3$ expression in H9c2 cells. Furthermore, these findings indicate that the effect of exogenous

S1P may be mediated by either Gi- or Gs-coupled receptors. The difference in the pattern of S1P receptor expression observed in primary cardiac muscle cells and H9c2 cells seems to not affect the cross-talk between S1P and RLX in term of CTFG release. However, the role of $S1P_3$ in primary cardiac muscle cells is worth investigating.

As reported in Nistri et al (15), RLX can promote the maturation of mouse neonatal cardiomyocytes in vitro. Based on this, we investigated whether S1P formation was also involved in this action. As revealed by [³H]thymidine incorporation (Table 3) and Western analysis of the key protein involved in myocardial differentiation, Cx43 (Figure 9), the synthesis of the bioactive lipid was required for RLX action. In particular, SphK activity inhibition resulted in 45% reduction in [³H]thymidine incorporation and approximately 70% reduction in Cx43 expression in primary cardiac muscle cells, indicating that SphK1/S1P axis is a crucial point in the biological action of RLX on cardiac muscle cells.

Discussion

This study offers new evidence for a previously unidentified intracellular signaling pathway activated in cardiac

H9c2 cardiomyoblasts, we observed that RLX, at concentrations similar to those previously reported to elicit specific responses in cardiac muscle cells (15, 48, 49), induces SM metabolism, SphK1 activation, and S1P production. Of note, the RLX-induced activation of SphK1 depends on ERK1/2 phosphorylation. In fact, pharmacological inhibition of ERK1/2, but not p38 MAPK, prevented RLX-mediated S1P formation.

The current findings indicate that the RLX-induced activation of S1P production is crucial for the capability of this hormone to induce an ECM-remodeling phenotype in cardiac muscle cells. Indeed, inhibition of the formation of SM metabolites abolished the increase in MMPs and decrease in TIMP-1 and CTGF expression induced by RLX in both primary cardiac muscle cells and H9c2 cardiomyoblasts. Of note, stimulation of ECM turnover is regarded as a major effect of RLX,

Figure 6. Effect of SphK, SMase, and S1P lyase inhibition and extracellular S1P addition on RLX-modulated TIMP-1 protein expression in H9c2 cells. Western blotting analysis of TIMP-1 protein expression. Cell lysates (15–30 μg) were obtained from H9c2 cells treated or not (vehicle) (A) for 30 minutes with the indicated agents (5μM compound II [iSK], 10μM GW9846, 6.5μM THI, or 1μM S1P) (B) and then with RLX (50 ng/mL) for 24 hours as reported in Figure 5. Band intensity, reported as relative percentage of the ratio between specific protein (TIMP-1)/β-actin), normalized to vehicle or to RLX value (set as 100), is shown in the graphics. A blot representative of at least 3 independent experiments with similar results is shown. Data are mean $\pm$ SEM (Student's t test; §, $P < .05$ vs RLX).
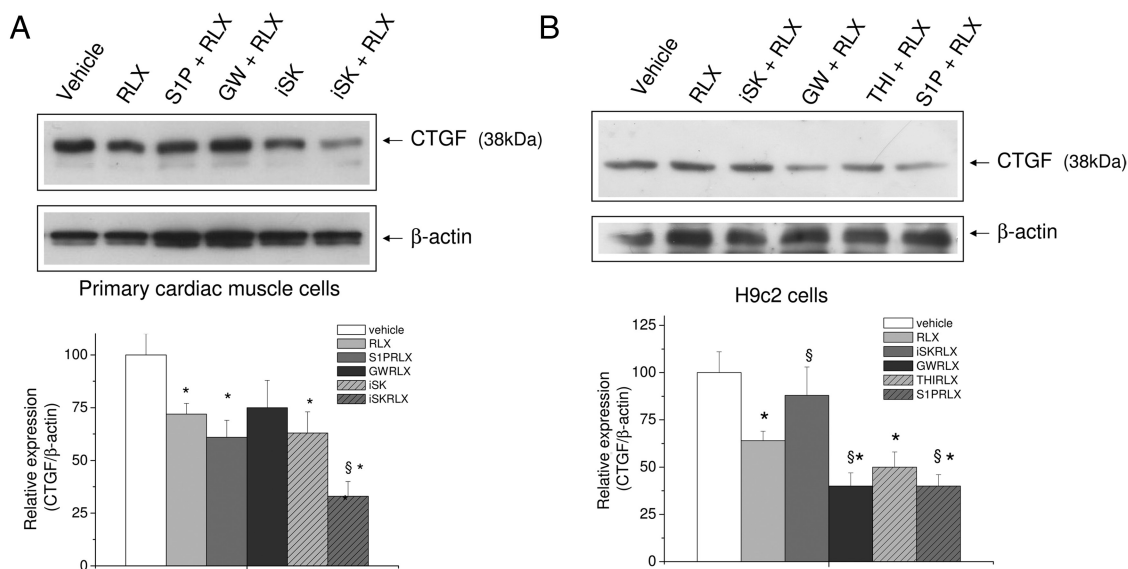
muscle cells by the cardiotropic hormone RLX, which involves the generation of the bioactive lipid S1P.

Using in vitro cultures of immature primary cardiac muscle cells from mouse neonatal hearts (15, 48) and rat

well supported by much of the recent literature (50, 51), acting through the upregulation of specific members of the MMP family: MMP-1, -3, -9, and -13 (14, 46). This action of RLX is mediated by its specific receptors, chiefly

Figure 7. Effect of SphK, SMase, and S1P lyase inhibition and extracellular S1P on CTGF expression in H9c2 cells. A and B, Western blot analysis of CTGF protein expression was performed by using cell lysates (15–30 μg) from untreated primary cardiac muscle cells (A) and H9c2 cardiomyoblasts (B) or treated for 30 minutes with indicated agents (5μM compound II [iSK], 10μM GW9846, 6.5μM THI, or 1μM S1P) and then with vehicle or RLX (50 ng/mL) for 24 hours. Band intensity, reported as relative percentage of the ratio between CTGF/β-actin, normalized to control, set as 100, is shown in the graphic. A blot representative of at least 3 independent experiments with similar results is shown. Data are mean $\pm$ SEM (Student's t test; *, $P < .05$ vs untreated cells (vehicle); §, $P < .05$ vs RLX).
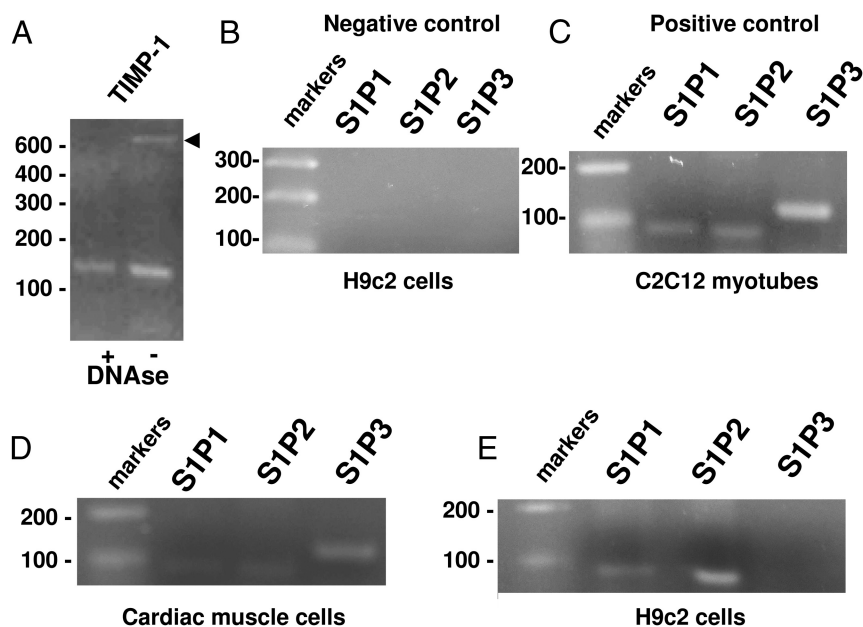
Figure 8. Expression of S1P receptor subtype in H9c2, primary cardiac muscle cells, and C2C12 myotubes. A–E, Representative agarose gels of amplified cDNA fragments. Total RNA was incubated with DNase and successively reverse transcribed. cDNAs were then amplified by PCR using specific primers for TIMP-1 (A) and $S1P_1$, $S1P_2$, and $S1P_3$ (B–E) as described in Materials and Methods. TIMP-1 amplification was performed by using untreated (−) or RNA treated with DNase (+) to eliminate DNA genomic contamination. B, Negative controls, consisting of no template (water) in each PCR. C, Positive controls consisting of cDNA obtained from murine C2C12 myotubes. D and E, cDNA amplification from reverse-transcribed RNA obtained from primary cardiac muscle (D) and H9c2 cells (E).

high-affinity RXFP1 (52). This acts as a Gs protein-coupled receptor and signals through adenylate cyclase to increase cAMP in different target cells (46). In particular, RXFP1 activation results in cAMP elevation through phosphatidylinositol-4,5-bisphosphate 3-kinase and calcium - and phorbol ester-insensitive zeta isozyme of protein kinase C pathways, (53). The RLX/ERK1/2 axis is also a classical downstream pathway of the cognate RLX receptor, RXFP1 (46, 49), here demonstrated to be expressed in primary cardiac muscle cells and H9c2 cardiomyoblasts. Therefore, the present study indicates that SphK1 and S1P can be considered a novel ERK1/2-dependent mechanism of the RLX/RXFP1 signaling pathway operating on cardiac muscle cells.

SLs are present in most if not all living organisms and cell types, where they represent a class of biomodulators of many cellular functions (1–4). Among the bioactive SLs derived by SM metabolism, S1P has emerged in the last decade as a crucial mediator of cardioprotection (3). Indeed, the level of S1P in plasma is drastically reduced early after MI, whereas the intracellular content of other SLs such as ceramide, sphinganine, and Sph are unchanged (54). Moreover, S1P mediates the survival of cardiomyocytes cultured under hypoxic conditions, as well as pre- and postconditioning in the heart subjected to ischemia/reperfusion injury (3). Despite the fact that both SphK1 and SphK2 isoforms catalyze the same reaction (3), it appears that the SphK1 isoform, predominantly localized in the cytosol and plasma membrane, plays a central role in cardioprotection (3). In line with this notion, SphK1 transgenic mice have been shown to develop progressive myocardial degeneration and fibrosis (55). On the other hand, there are conflicting reports on the role of SphK2 in ischemia-reperfusion injury (3), although the isoform, which accounts for nuclear and cardiac mitochondrial S1P generation, has also been shown to be necessary for successful ischemic pre- and postconditioning and cardioprotection (56). In the experimental conditions of the current study, SphK2 does not appear to be involved in the RLX signaling.

Table 2. S1P Receptor Subtype Expression in H9c2 Cells[a]

|	S1P1	S1P2	S1P3	GAPDH
Primary cardiac muscle cells				
Ct	17.44	17.97	17.28	13.26
ΔCt	4.18 ± 0.5	4.71 ± 0.6	4.02 ± 0.7	
H9c2 cells				
Ct	21.89	20.00		14.52
ΔCt	7.37 ± 0.8	5.48 ± 0.7		

[a] S1P receptor subtype expression was evaluated form total RNA of primary cardiac muscle and H9c2 cells after reverse transcription and real-time PCR amplification using specific primers as reported in Materials and Methods. ΔCt values are reported as mean ± SEM for independent experiments performed in duplicate.

Table 3. Effect of SphK Inhibition on [³H]Thymidine Incorporation in Primary Cardiac Muscle Cells[a]

Treatment (24 h)	[³H]Thymidine Incorporation (dpm/well)
Vehicle	3453 ± 288
RLX 50 ng/mL	2005 ± 256[b] (−42%)
RLX +iSK	3056 ± 510 (−12%)

[a] Primary cardiac muscle cell proliferation was determined at 24 hours from the addition of fresh culture medium (vehicle) or medium with RLX or medium with SphK inhibitor (iSK) for 30 minutes before hormone addition. [³H]Thymidine was added to the medium for the last 2 hours. The β-counts (dpm, disintegrations per minute) per well are reported as mean ± SEM for at least 3 independent experiments performed in duplicate.

[b] Significance of differences (one-way ANOVA, n = 3): $P < .05$. Note no significant change was observed in the presence of iSK alone.
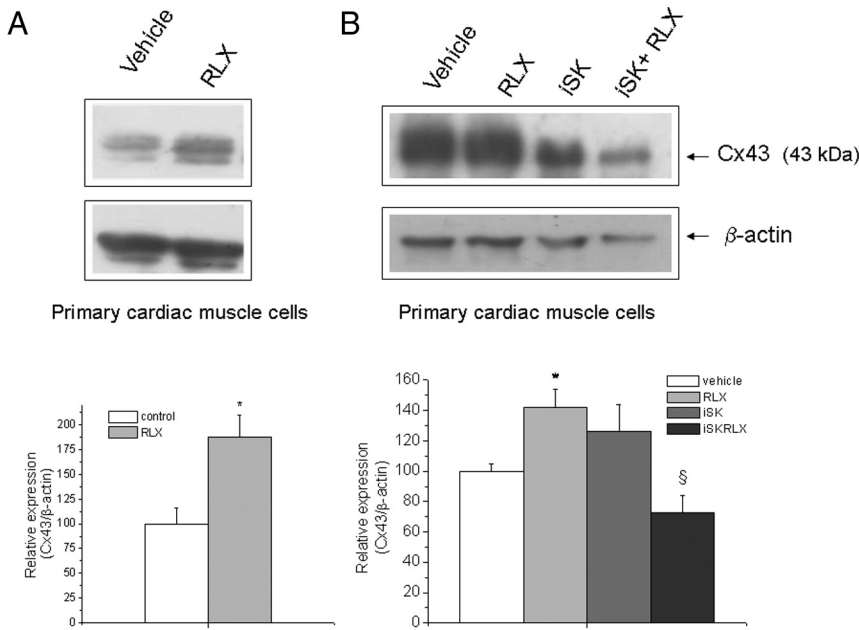
Figure 9. Effect of SL metabolism inhibition and extracellular S1P addition on Cx43 expression in primary cardiac muscle cells and H9c2 cells. A and B, Western blot analysis of Cx43 protein expression. Cell lysates (10 μg) from primary cardiac muscle cells were treated for 30 minutes without (A) or with the indicated agents (5μM compound II [iSK], 10μM GW9846, 6.5μM THI, or 1μM S1P) (B) and then with RLX (50 ng/mL) for 24 hours. Quantification of band intensity, shown in the graphic, is reported as ratio between overall Cx43/β-actin, and relative to control normalized to 100. Data are mean $\pm$ SEM (n = 3, Student's t test; *, $P < .05$ vs untreated cells (vehicle); §, $P < .05$ vs RLX).

Interestingly, in recent years, numerous studies have established that bioactive lipids can modulate fibrogenesis in various organs, including the lung, skin, liver, heart, and eye, by influencing both the onset and the progression of the pathological accumulation of myofibroblasts and ECM (57). The rising interest in the ability of SLs, in particular S1P, to reduce tissue fibrosis is based on their ability to regulate key cellular processes involved in tissue responses to injury (4) such as apoptosis, fibro-

blast migration and myofibroblast differentiation, and TGF-β signaling. The present findings confirm the ability of bioactive SLs to promote ECM remodeling by modulating the release of MMPs and add a novel piece of knowledge demonstrating that SLs are also required for the profibrotic CTGF expression elicited by RLX in cardiomyoblasts. CTGF has been recently identified as a key factor in heart remodeling (58), because it regulates several cellular processes, such as ECM deposition, wound repair, and angiogenesis as well as cardiac cell migration, differentiation, and survival (28). Besides its major role in tissue fibrosis, CTGF has also been shown to compete with Wnt family members and to synergize with TGF-β, supporting a role for this cytokine as an endogenous coordinator of multiple signaling pathways (28, 29). A single piece of evidence supports a role of S1P in the downregulation of CTGF at the mRNA level in mesangial cells (59). Therefore, the current novel findings that RLX can decrease CTGF expression through SL-mediated mechanisms appears particularly relevant, because they offer new perspectives for antifibrotic therapeutic approaches

Although we did not specifically investigate the action of RLX on S1P receptor subtype-mediated signaling, the current data indicate that primary cardiac muscle cells and H9c2 cells expressed several S1P receptor subtypes similarly to other skeletal muscle cells, such as C2C12 myotubes (60). Extracellular S1P was able to inhibit the effects of RLX on the release of MMPs and potentiate hormone action on CTGF expression likely through S1P$_1$, S1P$_2$, and/or S1P$_3$. In the heart, binding of S1P to its specific receptors (61) activates downstream signaling mechanisms leading to modulation of cell survival and fibrosis (62, 63). Moreover, diminished circulating S1P levels were observed in various human diseases characterized by tissue fibrosis (64), and neutralization of S1P with specific anti-S1P antibod-
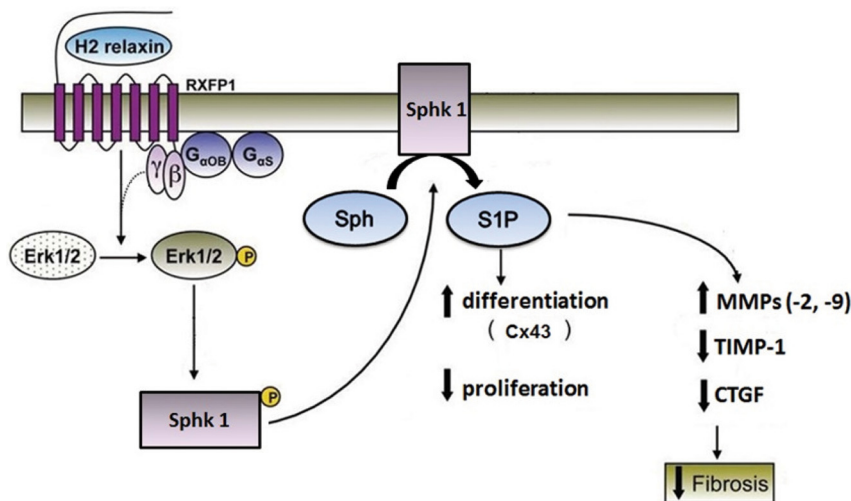
Figure 10. Scheme of the antifibrotic and procardiomyogenic RLX signaling involving SphK/S1P axis in cardiac cells.

ies significantly reduced TGFβ-stimulated collagen production (62).

Because established tissue fibrosis is usually irreversible, preventative strategies capable of interrupting the upstream biological processes that contribute to fibrogenesis can have a major therapeutic impact. In this view, a possible cross-talk between the signaling pathways triggered by activation of the specific RLX and S1P receptors may be worthy of further investigation.

Our study also provides circumstantial evidence that the SphK1/S1P axis can play an important role in the differentiation of cardiac muscle precursors induced by RLX. In fact, we observed that pharmacological inhibition of SphK counteracted the effect of RLX on Cx43 expression and cell cycle arrest, suggesting that an SphK1/S1P-mediated signaling pathway is involved in the modulation of the cardiomyogenic program operated by RLX.

Conclusions

Taken together, the key findings of this study indicate that RLX promotes an ECM-remodeling phenotype and the maturation of cardiac muscle cells through the activation of endogenous S1P production and SM metabolism (Figure 10). This notion can be relevant to heart pathophysiology. In fact, RLX can be rightfully included among the cardiotropic factors capable of inducing favorable myocardial remodeling in the diseased heart (23, 47). In this view, human recombinant H2 RLX was found effective in improving the clinical outcome and overall survival of patients with acute heart failure (25, 26).

Thus, increasing the knowledge of the mechanisms involved in increased ECM turnover, as well as in enhanced self-renewal and in situ differentiation of resident myocardial progenitor cells, is helpful to better understand the intrinsic repair mechanisms of the failing heart (26) and can provide a mechanistic background to RLX-based therapeutic strategies in MI (65).

Address all correspondence and requests for reprints to: Prof Elisabetta Meacci, Department of Biomedical, Experimental, and Clinical Sciences, Research Unit of Biochemical Sciences and Molecular Biology, Viale GB Morgagni 50, University of Florence, 50134 Florence, Italy. E-mail: elisabetta.meacci@unifi.it.

References

1. **Fyrst H, Saba JD.** An update on sphingosine-1-phosphate and other sphingolipid mediators. *Nat Chem Biol*. 2010;6:489–497.
2. **Bartke N, Hannun YA.** Bioactive sphingolipids: metabolism and function. *J Lipid Res*. 2009;50:S91–S96.
3. **Maceyka M, Harikumar KB, Milstien S, Spiegel S.** Sphingosine-1-phosphate signaling and its role in disease. *Trends Cell Biol*. 2012;22:50–60.
4. **Hannun YA, Obeid LM.** Principles of bioactive lipid signalling: lessons from sphingolipids. *Nat Rev Mol Cell Biol*. 2008;9:139–150.
5. **Gault CR, Obeid LM, Hannun YA.** An overview of sphingolipid metabolism: from synthesis to breakdown. *Adv Exp Med Biol*. 2010;688:1–23.
6. **Wu WT, Chen CN, Lin CI, Chen JH, Lee H.** Lysophospholipids enhance matrix metalloproteinase-2 expression in human endothelial cells. *Endocrinology*. 2005;146:3387–3400.
7. **Annabi B, Thibeault S, Lee YT, et al.** Matrix metalloproteinase regulation of sphingosine-1-phosphate-induced angiogenic properties of bone marrow stromal cells. *Exp Hematol*. 2003;31:640–649.
8. **Buisson-Legendre N, Bernard P, Bobichon H, et al.** Involvement of the 92-kDa gelatinase (matrix metalloproteinase-9) in the ceramide-mediated inhibition of human keratinocyte growth. *Biochem Biophys Res Commun*. 1999;260:634–640.
9. **Spinale FG.** Myocardial matrix remodeling and the matrix metalloproteinases: influence on cardiac form and function. *Physiol Rev*. 2007;87:1285–1342.
10. **Bergers G, Brekken R, McMahon G, Vu TH, Itoh T.** Matrix metalloproteinase-9 triggers the angiogenic switch during carcinogenesis. *Nat Cell Biol*. 2000;2:737–744.
11. **Schulz R.** Intracellular targets of matrix metalloproteinase-2 in cardiac disease: rationale and therapeutic approaches. *Annu Rev Pharmacol Toxicol*. 2007;47:211–242.
12. **Matsumoto Y, Park IK, Kohyama K.** Matrix metalloproteinase (MMP)-9, but not MMP-2, is involved in the development and progression of C protein-induced myocarditis and subsequent dilated cardiomyopathy. *J Immunol*. 2009;183:4773–4781.
13. **Matsumura S, Iwanaga S, Mochizuki S, Okamoto H, Ogawa S, Okada Y.** Targeted deletion or pharmacological inhibition of MMP-2 prevents cardiac rupture after myocardial infarction in mice. *J Clin Invest*. 2005;115:599–609.
14. **Samuel CS, Lekgabe ED, Mookerjee I.** The effects of relaxin on extracellular matrix remodeling in health and fibrotic disease. *Adv Exp Med Biol*. 2007;612:88–103.
15. **Nistri S, Pini A, Sassoli C, et al.** Relaxin promotes growth and maturation of mouse neonatal cardiomyocytes in vitro: clues for cardiac regeneration. *J Cell Mol Med*. 2012;16:507–519.
16. **Wilkinson TN, Speed TP, Tregear GW, Bathgate RA.** Evolution of the relaxin-like peptide family. *BMC Evol Biol*. 2005;5:14.
17. **Unemori EN, Pickford LB, Salles AL, et al.** Relaxin induces an extracellular matrix-degrading phenotype in human lung fibroblasts in vitro and inhibits lung fibrosis in a murine model in vivo. *J Clin Invest*. 1996;98:2739–2745.
18. **Samuel CS, Royce SG, Chen B, et al.** Relaxin family peptide receptor-1 protects against airway fibrosis during homeostasis but not against fibrosis associated with chronic allergic airways disease. *Endocrinology*. 2009;150:1495–1502.
19. **Heeg MH, Koziolek MJ, Vasko R, et al.** The antifibrotic effects of

relaxin in human renal fibroblasts are mediated in part by inhibition of the Smad2 pathway. *Kidney Int*. 2005;68:96–109.

20. **Mookerjee I, Hewitson TD, Halls ML, et al.** Relaxin inhibits renal myofibroblast differentiation via RXFP1, the nitric oxide pathway, and Smad2. *FASEB J*. 2009;23:1219–1229.

21. **Dschietzig T, Richter C, Bartsch C, et al.** The pregnancy hormone relaxin is a player in human heart failure. *FASEB J*. 2001;15:2187–2195.

22. **Nistri S, Bigazzi M, Bani D.** Relaxin as a cardiovascular hormone: physiology, pathophysiology and therapeutic promises. *Cardiovasc Hematol Agents Med Chem*. 2007;5:101–108.

23. **Du XJ, Bathgate RA, Samuel CS, Dart AM, Summers RJ.** Cardiovascular effects of relaxin: from basic science to clinical therapy. *Nat Rev Cardiol*. 2010;7:48–58.

24. **Du XJ, Samuel CS, Gao XM, Zhao L, Parry LJ, Tregear GW.** Increased myocardial collagen and ventricular diastolic dysfunction in relaxin deficient mice: a gender-specific phenotype. *Cardiovasc Res*. 2003;57:395–404.

25. **Teerlink JR, Metra M, Felker GM, et al.** Relaxin for the treatment of patients with acute heart failure (Pre-RELAX-AHF): a multicentre, randomised, placebo-controlled, parallel-group, dose-finding phase IIb study. *Lancet*. 2009;373:1429–1439.

26. **Teichman SL, Unemori E, Teerlink JR, Cotter G, Metra M.** Relaxin: review of biology and potential role in treating heart failure. *Curr Heart Fail Rep*. 2010;7:75–82.

27. **Frangogiannis NG.** Matricellular proteins in cardiac adaptation and disease. *Physiol Rev*. 2012;92:635–688.

28. **Perbal B.** CCN proteins: A centralized communication network. *J Cell Commun Signal*. 2013;7:169–177.

29. **Daniels A, van Bilsen M, Goldschmeding R, van der Vusse GJ, van Nieuwenhoven FA.** Connective tissue growth factor and cardiac fibrosis. *Acta Physiol (Oxf)*. 2009;195:321–338.

30. **Formigli L, Perna AM, Meacci E, et al.** Paracrine effects of transplantated myoblasts and relaxin on post-infarction heart remodelling. *J Cell Mol Med*. 2007;11:1087–1100.

31. **Airola MV, Hannun YA.** Sphingolipid metabolism and neutral sphingomyelinases. *Handb Exp Pharmacol*. 2013;215:57–76.

32. **Luberto C, Hassler DF, Signorelli P, et al.** Inhibition of tumor necrosis factor-induced cell death in MCF7 by a novel inhibitor of neutral sphingomyelinase. *J Biol Chem*. 2002;277:41128–41139.

33. **French KJ, Schrecengost RS, Lee BD, et al.** Discovery and evaluation of inhibitors of human sphingosine kinase. *Cancer Res*. 2003;63:5962–5969.

34. **Kleinjan A, van Nimwegen M, Leman K, Hoogsteden HC, Lambrecht BN.** Topical treatment targeting sphingosine-1-phosphate and sphingosine lyase abrogates experimental allergic rhinitis in a murine model. *Allergy*. 2013;68:204–212.

35. **Meacci E, Nuti F, Donati C, Cencetti F, Farnararo M, Bruni P.** Sphingosine kinase activity is required for myogenic differentiation of C2C12 myoblasts. *J Cell Physiol*. 2008;214:210–220.

36. **Sassoli C, Formigli L, Squecco R, Zecchi-Orlandini S, Francini F, Meacci E.** Effects of S1P on skeletal muscle repair/regeneration during eccentric contraction. *J Cell Mol Med*. 2010;10:1111–1125.

37. **Meacci E, Bini F, Battistini C.** Sphingosine-1-phosphate signaling in skeletal muscle cells. *Methods Mol Biol*. 2012;876:155–165.

38. **De Palma C, Meacci E, Perrotta C, Bruni P, Clementi E.** Endothelial nitric oxide synthase activation by tumor necrosis factor alpha through receptors: a novel pathway relevant to the pathophysiology of endothelium neutral sphingomyelinase 2, sphingosine kinase 1, and sphingosine 1 phosphate. *Arterioscler Thromb Vasc Biol*. 2006;26:99–105.

39. **Formigli L, Sassoli C, Squecco R, Zecchi-Orlandini S, Francini F, Meacci E.** Regulation of transient receptor potential channel 1 (TRPC1) by sphingosine-1-phosphate in C2C12 myoblasts and its relevance for a role of mechanotransduction in skeletal muscle differentiation. *J Cell Sci*. 2009;122(Pt 9):1322–1333.

40. **Meacci E, Bini F, Sassoli C, et al.** Functional interaction between

41. **Squecco R, Sassoli C, Nuti F, et al.** Sphingosine 1-phosphate induces myoblast differentiation through Cx43 protein expression: a role for a gap junction-dependent and -independent function. *Mol Biol Cell*. 2006;17:4896–4910.

42. **Bini F, Frati A, Garcia-Gil M, et al.** New signalling pathway involved in the antiproliferative action of Vitamin D$_3$ and its structural analogues in human neuroblastoma cells. A role for ceramide kinase/ceramide 1-phosphate axis. *Neuropharmacology*. 2012;63:524–537.

43. **Lucki NC, Sewer MB.** The interplay between bioactive sphingolipids and steroid hormones. *Steroids*. 2010;75:390–399.

44. **Formigli L, Zecchi-Orlandini S, Meacci E, Bani D.** Skeletal myoblasts for heart regeneration and repair: state of the art and perspectives on the mechanisms for functional cardiac benefits. *Curr Pharm Des*. 2010;16:915–928.

45. **Chow BS, Chew EG, Zhao C, Bathgate RA, Hewitson TD, Samuel CS.** Relaxin signals through a RXFP1 pERK-nNOS-NO-cGMP-dependent pathway to up-regulate matrix metalloproteinases: the additional involvement of iNOS. *PLoS One*. 2012;7:e42714.

46. **Ahmad N, Wang W, Nair R, Kapila S.** Relaxin induces matrix-metalloproteinases-9 and -13 via RXFP1: induction of MMP-9 involves the PI3K, ERK, Akt and PKC-ζ pathways. *Mol Cell Endocrinol*. 2012;363:46–61.

47. **Bani D, Bigazzi M.** Relaxin as a cardiovascular drug: a promise kept. *Curr Drug Saf*. 2011;6:324–328.

48. **Devic E, Xiang Y, Gould D, Kobilka B.** Beta-adrenergic receptor subtype-specific signaling in cardiac myocytes from beta(1) and beta (2) adrenoceptor knockout mice. *Mol Pharmacol*. 2001;60:577–583.

49. **van der Westhuizen ET, Halls ML, Samuel CS, et al.** Relaxin family peptide receptors–from orphans to therapeutic targets. *Drug Discov Today*. 2008;13:640–651.

50. **Zhao L, Roche PJ, Gunnersen JM, et al.** Mice without a functional relaxin gene are unable to deliver milk to their pups. *Endocrinology*. 1999;140:445–453.

51. **Lekgabe ED, Kiriazis H, Zhao C, et al.** Relaxin reverses cardiac and renal fibrosis in spontaneously hypertensive rats. *Hypertension*. 2005;46:412–418.

52. **Bathgate RA, Halls ML, van der Westhuizen ET, Callander GE, Kocan M, Summers RJ.** Relaxin family peptides and their receptors. *Physiol Rev*. 2013;93:405–480

53. **Halls ML, Papaioannou M, Wade JD, Evans BA, Bathgate RA, Summers RJ.** RXFP1 couples to the Galpha-Gbetagamma-PI3K-PKCzeta pathway via the final 10 amino acids of the receptor C-terminal tail. *Ann N Y Acad Sci*. 2009;1160:117–120.

54. **Knapp M, Baranowski M, Czarnowski D, et al.** Plasma sphingosine-1-phosphate concentration is reduced in patients with myocardial infarction. *Med Sci Monit*. 2009;15:CR490–CR493.

55. **Takuwa N, Ohkura S, Takashima S, et al.** S1P3-mediated cardiac fibrosis in sphingosine kinase 1 transgenic mice involves reactive oxygen species. *Cardiovasc Res*. 2010;85:484–493.

56. **Gomez L, Paillard M, Price M, Chen Q, Teixeira G, Spiegel S, Lesnefsky EJ.** A novel role for mitochondrial sphingosine-1-phosphate produced by sphingosine kinase-2 in PTP-mediated cell survival during cardioprotection, *Basic Res Cardiol*. 2011;106:1341–1353.

57. **Schwalm S, Pfeilschifter J, Huwiler A.** Sphingosine-1-phosphate: a Janus-faced mediator of fibrotic diseases. *Biochim Biophys Acta*. 2013;1831:239–250.

58. **Matsui Y, Sadoshima J.** Rapid upregulation of CTGF in cardiac myocytes by hypertrophic stimuli: implication for cardiac fibrosis and hypertrophy. *J Mol Cell Cardiol*. 2004;37:477–481.

59. **Katsuma S, Hada Y, Shiojima S, et al.** Transcriptional profiling of gene expression patterns during sphingosine 1-phosphate-induced

TRPC1 channel and connexin-43 protein: a novel pathway underlying S1P action on skeletal myogenesis. *Cell Mol Life Sci*. 2010;67:4269–4285.

mesangial cell proliferation. *Biochem Biophys Res Commun*. 2003; 300:577–584.

60. **Meacci E, Cencetti F, Donati C, et al.** Down-regulation of EDG5/ S1P2 during myogenic differentiation results in the specific uncoupling of sphingosine 1-phosphate signalling to phospholipase D. *Biochim Biophys Acta*. 2003;1633:133–142.

61. **Bünemann M, Brandts B, zu Heringdorf DM, van Koppen CJ, Jakobs KH, Pott L.** Activation of muscarinic K^+ current in guinea-pig atrial myocytes by sphingosine-1-phosphate. *J Physiol*. 1995; 489:701–707.

62. **Gellings Lowe N, Swaney JS, Moreno KM, Sabbadini RA.** Sphingosine-1-phosphate and sphingosine kinase are critical for transforming growth factor-beta-stimulated collagen production by cardiac fibroblasts. *Cardiovasc Res*. 2009;82:303–312.

63. **Shea BS, Brooks SF, Fontaine BA, Chun J, Luster AD, Tager AM.** Prolonged exposure to sphingosine 1-phosphate receptor-1 agonists exacerbates vascular leak, fibrosis, and mortality after lung injury. *Am J Respir Cell Mol Biol*. 2010;43:662–673.

64. **Ikeda H, Ohkawa R, Watanabe N, et al.** Plasma concentration of bioactive lipid mediator sphingosine 1-phosphate is reduced in patients with chronic hepatitis C. *Clin Chim Acta*. 2010;411:765–770.

65. **Waeber C, Walther T.** Sphingosine-1-phosphate as a potential target for the treatment of myocardial infarction. *Circ J*. 2014;78:795–802.